Journal of Solid State Chemistry **166,** 320–329 (2002)
doi:10.1006/jssc.2002.9594

The Local Uranium Environment in Cesium Uranates: A Combined XPS, XAS, XRD, and Neutron Diffraction Analysis

Sven Van den Berghe,*[,1] M. Verwerft,* J.-P. Laval,† B. Gaudreau,† P. G. Allen,‡ and A. Van Wyngarden‡

*SCK·CEN, Boeretang 200, B-2400 Mol, Belgium; †Université de Limoges, SPCTS UMR-CNRS no 6638, Av. Albert-Thomas, 87060 Limoges Cedex, France; ‡Seaborg Institute, Lawrence Livermore National Laboratory, P.O. Box 808 MS L-231, Livermore, California 94551

Received September 17, 2001; in revised form March 8, 2002; accepted March 22, 2002

The cesium uranates Cs_2UO_4, $Cs_2U_2O_7$, $Cs_4U_5O_{17}$ and $Cs_2U_4O_{12}$ were studied using X-ray Diffraction (XRD), neutron diffraction, X-ray Photoelectron Spectroscopy (XPS) and X-ray Absorption Spectroscopy (XAS) in an attempt to couple the crystallographic structure to the uranium valence state using the local uranium environment. The diffraction spectra were used for Rietveld refinement to determine the atomic positions and interatomic distances. These distances were subsequently used in Bond Valence Sum (BVS) calculations to determine the uranium valences. The XAS spectra give direct information on the local uranium environment regarding the U–O distances and the arrangement of the oxygen atoms around the central uranium. The difference between the monovalent uranates and the multivalent $Cs_2U_4O_{12}$ is clearly established in all spectra, as well as in the crystal structures. The different valences present can be assigned to individual uranium lattice sites, but some amount of disorder is required to balance the charges. © 2002 Elsevier Science (USA)

Key Words: **cesium uranates; XPS; EXAFS; XANES; XRD; neutron powder diffraction; Rietveld.**

1. INTRODUCTION

Recently, a study of the X-ray Photoelectron Spectroscopy (XPS) on a set of cesium uranates was published (1). Some of the uranates dealt with in that paper ($Cs_2U_2O_7$, $Cs_4U_5O_{17}$ and $Cs_2U_4O_{12}$) have now been further explored in an extensive series of measurements, including X-ray diffraction (XRD), neutron diffraction, extended X-ray Absorption Fine Structure (EXAFS) and X-ray Absorption Near-Edge Spectroscopy (XANES) measurements, to study the local environment of the uranium atoms. This can provide us with a link between the crystallographic structure and uranium valence states of these uranates. At the time the previous article was written, XPS measurements on Cs_2UO_4 were not yet included because of its hygroscopic properties, while we have been able to perform them now.

From the X-ray and neutron diffraction data, the crystal structure of the cesium uranates was re-investigated. Van Egmond *et al.* have studied the crystal structures of the cesium uranates in 1976 (2). In that case, neutron diffraction experiments were only performed on $Cs_2U_2O_7$. The crystal structure of this compound was re-determined by Mijlhoff *et al.* from electron and neutron diffraction (3) when it was realized that the two phases postulated by Van Egmond are, in fact, only one phase and its hydrated form. For $Cs_2U_2O_7$, we have used the crystal structure as determined in (3). For $Cs_4U_5O_{17}$ and $Cs_2U_4O_{12}$, new Rietveld refinements were performed on the basis of the combined data provided by X-ray and neutron diffraction, while for Cs_2UO_4 only neutron diffraction data were used. The determined atomic positions and interatomic distances are reproduced in this article. A complete crystallochemical discussion of $Cs_2U_4O_{12}$ and its relation to homologous structures, will be published separately (4).

To the knowledge of the authors, no X-ray Absorption Spectroscopy (XAS) measurements of cesium uranates have been published. The XAS spectra provide additional information on the local uranium environment, notably on the U–O distances and the arrangement of the oxygen atoms around the central uranium. Deconvolution of the XANES spectrum can help to confirm the distribution of the different uranium valences present in the case of a multivalent compound. The mathematical modeling of the EXAFS results serves as a tool to visualize the mean local environment of the uranium atoms in the sample.

The information extracted from the XPS is discussed in (1). The relevant data will be repeated in the text. For Cs_2UO_4, the complete discussion can be found below. A

[1] To whom correspondence should be addressed. E-mail: svdbergh@sckcen.be.

0022-4596/02 $35.00

method to relate the crystal structure to the chemical valences is the Bond Valence Sum (BVS). It will be shown that the general approach to BVS calculations as published by Brown *et al.* (5) is not suitable for all uranium compounds and that the more specific approach of Zachariasen (6) gives better agreement.

The BVS are a concise, empirical way of treating all U–O bond lengths in a U environment. For U compounds, several studies have shown the influence of the U–O bond length on the XPS spectral features. It was demonstrated that the splitting of the U6$p_{3/2}$ due to ligand electric fields is determined by the U–O distance (7, 8). The O1*s* position in a large set of alkali earth-metal uranates was also shown to be closely related to the U–O bond length (9).

2. EXPERIMENTAL AND DATA ANALYSIS

The preparation of the cesium uranates was described in (1). In view of their hygroscopic nature, the samples were stored in vacuum on a bed of P_2O_5.

For neutron diffraction, the powders were loaded in vanadium containers that were closed during the measurements. The spectra from 0° to 160° 2θ were recorded at the D2B high-resolution/high-flux powder diffractometer at the Institut Laue-Langevin in Grenoble, France. The goniometer was operated in the high-flux mode (neutron wavelength of 1.594 Å). Each sample was passed for 3–4 h.

The X-ray diffractograms for some uranates ($Cs_2U_4O_{12}$ and $Cs_4U_5O_{17}$) were recorded at the university of Limoges on a Siemens D5000 diffractometer, using non-monochromatic Cu$K\alpha$ radiation and equipped with a secondary monochromator. For Cs_2UO_4, the diffraction spectra were recorded at the SCK·CEN using a Philips X'Pert Pro, also with non-monochromatic Cu$K\alpha$ radiation and a back-monochromator. Both goniometers were carefully aligned before the spectra were recorded. The data were recorded over more than 48 h for each compound. The spectra were analyzed and compared to reference spectra from the JCPDS-database (Pattern 29-0429 for Cs_2UO_4, 29-0431 for $Cs_2U_2O_7$, 29-0432 for $Cs_2U_4O_{12}$ and 29-0439 for $Cs_4U_5O_{17}$). From these comparisons, the purity of the powders could be verified.

Neutron and X-ray diffraction data were then used in the FullProf (10) Rietveld refinement program to determine the crystal structures of the various uranates (4). The crystal structures, as determined by Van Egmond (2), were used as a starting point for the analysis. For $Cs_2U_4O_{12}$, however, changes had to be made to the space group and atom positions had to be determined ab initio. The pseudo-Voigt peak shape was selected for these refinements. For $Cs_2U_2O_7$, the crystal structure refinement resulting from the recent neutron diffraction study was used (3). R_{Bragg} values for all refinements were below 5% (R_p values indicated in tables), except in the case of Cs_2UO_4, where some unidentified impurities in the sample (possibly the hydrated form of Cs_2UO_4) interfered with the refinement, producing a R_{Bragg} factor of 6.39%. Because the impurity lines interfere only weakly with the reflections of the desired structure, the resulting atomic positions can still be regarded as reliable. Cs_2UO_4 was refined on the basis of the neutron data alone, because its hygroscopic nature is not compatible with X-ray diffraction experiments of over 48 h.

For the XAS measurements, a precisely weighted quantity of each uranate was intimately mixed with boron nitride (BN) and loaded in aluminum sample holders that were subsequently sealed. Uranium L_{III}-edge X-ray absorption spectra were collected on beam line 4-1 at the Stanford Synchrotron Radiation Laboratory (SSRL) using a Si(2 2 0) double-crystal monochromator. The beam size was typically 0.5 mm (vertical) ×10 mm (horizontal). All spectra were collected in transmission mode at room temperature using argon-filled ionisation chambers. The spectra were energy calibrated by simultaneous measurement of the transmission spectrum of UO_2(s), where the energy of the first inflection point for the reference sample absorption edge, E_r, was defined as 17166.0 eV. Rejection of higher-order harmonics in the beam was achieved by detuning θ, the angle between monochromator crystals, so that the incident flux was reduced to 50% of maximum.

The XANES and EXAFS data were extracted from the raw absorption spectra by standard methods described elsewhere (11), using the suite of programs, EXAFSPAK, developed by Graham George of SSRL. Non-linear least-squares curve fitting analysis was performed using EXAFSPAK to fit the raw k_3-weighted data based on neighboring shells of atoms. Backscattering phases and amplitudes were also calculated from model compounds using FEFF8.1 (12). Input files for FEFF8.1 were prepared using the structural modeling code ATOMS 2.46b (13). The crystal structure datasets for the different compounds were used to calculate phase and amplitude corrections for all uranium-backscatter interactions for the non-linear least-squares EXAFS fitting procedure.

The photoelectron spectra were recorded at the university of Brussels (VUB) in Belgium. The experimental conditions used for the XPS measurements are described in (1). For Cs_2UO_4, similar conditions were used, but the sample was stored in the vacuum airlock of the spectrometer for one night to avoid substantial degassing of this hygroscopic compound in the analysis chamber. It is important to mention that the C1*s* peak position as used for charging correction in (1) should be increased by 0.4 eV. The value of 284.6 eV as used in (1) is more suitable for carbon on (noble) metals, while the value of 285.0 eV is more appropriate for these ceramic samples. The binding energy values quoted in this article have been corrected on the basis of 285.0 eV as the C1*s* position.

3. RESULTS

The atomic positions resulting from the refinements were used to determine the local uranium environments in every compound. More specifically, the U–O bond lengths were used in the formula for the BVS. In these calculations, we have used the Zachariasen (6) approach, based on his bond length–bond strength formula. The bond strength or bond valence s_{ij} is defined as $s_{ij} = e^{R_0 - R_{ij}/b}$ and the BVS $z_j = \sum_i s_{ij}$ in which b is a constant and depends on the atom pair under consideration. R_{ij} is the bond length and z_j is the oxidation state. This definition has been used by Brown and Altermatt (5), as well as by Brese and O'Keeffe (14), to determine R_0 for a range of atom pairs by direct determination from the known crystal structures or by interpolation. They use the constant value of 0.37 for b for all element pairs. However, these authors also point out that, although their formula gives a good indication for compounds of all elements, it is always better to use a more specific set of values for R_0 and b that are optimized for treating a specific system. Zachariasen (6) has published values for R_0 and b in the case of U–O bonds and we will use his values in this paper. The parameters that were used, are $R_0 = 2.083$ Å for U^{6+} and $R_0 = 2.10$ Å for U^{5+}. For b, a value of 0.35 is used, except where the bond valence $s > 1$, then $b = 0.35 + 0.12(s - 1)$. In this last case, the actual value of s is calculated iteratively.

The resulting BVS were then compared to the XPS results and valences were attributed to each uranium atom in the crystal structure for the mixed valence compound. The uranium environments as determined in the refinements were checked against the XANES and EXAFS data.

3.1. Monovalent (Valence VI) Uranates: Cs_2UO_4, $Cs_2U_2O_7$, and $Cs_4U_5O_{17}$

The final refined atomic positions are shown in Tables 1 and 3, while in Table 2, the results of the structure refinement of Mijlhof *et al.* are reproduced. From the U–O distances calculated after refinement of the structures (see Table 4), it can be deduced that the monovalent uranates show "uranyl"-type uranium environments. The "uranyl"-environment consists of two short U–O bond lengths (1.7–2.0 Å), which will be called the axial bonds and longer equatorial U–O bond lengths (> 2.0 Å) for the four or five other ligands surrounding the central uranium atom. These oxygen atoms are then found in a close to planar arrangement, perpendicular to the linear O–U–O configuration formed by the uranyl ion. The uranyl ion is often denoted as UO_2^{2+}. In a free uranyl ion, the axial bond lengths have been calculated to be 1.7–1.8 Å (15) and in γ-UO_3 the axial bonds have lengths of 1.797 Å. The uranyl groups in the cesium uranates have generally longer axial U–O bonds: 1.825–1.866Å in $Cs_4U_5O_{17}$, 1.807–1.835 Å in $Cs_2U_2O_7$ and 1.914 Å in Cs_2UO_4, as can be seen from Table 5. For $Cs_4U_5O_{17}$, only the seven-coordinated uranium atom U1 has a short uranyl bond of 1.785 Å, but the general tendency is for the cesium uranates to have

TABLE 1
Final Refined Lattice Parameters, Fractional Coordinates, and Isotropic Temperature Factors B_{iso} of Cs_2UO_4

Atom	Site	x/a	y/a	z/c	B_{iso} (Å^2)
Cs	4*e*	0	0	0.3439(2)	1.94(6)
U	2*a*	0	0	0	1.26(4)
O1	4*c*	0	$\frac{1}{2}$	0	1.67(5)
O2	4*e*	0	0	0.1291(2)	1.87(6)

Note. Space group $I4/mmm$ (No.139), tetragonal; cell parameters: $a = 4.391(1)$ Å, $c = 14.823(1)$ Å; $R_B = 6.39\%$, $R_p = 4.92\%$ (neutron diffraction only).

TABLE 2
Lattice Parameters, Fractional Coordinates, and Isotropic Temperature Factors B_{iso} of $Cs_2U_2O_7$ (after (3))

Atom	Site	x/a	y/b	z/c	B_{iso} (Å^2)
Cs1	4*i*	0.3994(3)	0	0.5868(7)	1.29(12)
U1	4*i*	0.1469(3)	0	−0.0076(5)	0.02(7)
O1	4*i*	0.2003(4)	0	0.2562(7)	1.59(14)
O2	4*i*	0.4108(4)	$\frac{1}{2}$	0.2755(6)	1.31(14)
O3	4*i*	0.3104(3)	0	0.0030(6)	0.64(18)
O4	2*a*	0	0	0	0.83(24)

Note. Space group $C2/m$ (No.12), monoclinic; cell parameters: $a = 14.5293(9)$ Å, $b = 4.3233(3)$ Å, $c = 7.4899(5)$ Å, $\beta = 113.852(1)^\circ$; $R_p = 3.24\%$ (neutron diffraction only, no R_{Bragg} value). Values taken from (3).

TABLE 3
Final Refined Lattice Parameters, Fractional Coordinates, and Isotropic Temperature Factors B_{iso} of $Cs_4U_5O_{17}$

Atom	Site	x/a	y/b	z/c	B_{iso} (Å^2)
Cs1	8*d*	0.3087(3)	0.3023(8)	0.4457(4)	1.70(12)
Cs2	8*d*	0.0552(4)	0.2721(10)	0.4701(4)	1.94(13)
U1	4*c*	$\frac{1}{2}$	0.1318(7)	$\frac{1}{4}$	0.84(10)
U2	8*d*	0.1038(2)	0.0791(5)	0.2075(2)	0.86(6)
U3	8*d*	0.3121(2)	0.0274(4)	0.1871(2)	0.60(5)
O1	4*c*	0	−0.0368(19)	$\frac{1}{4}$	0.88(21)
O2	8*d*	0.0786(5)	0.0739(15)	0.0868(6)	1.54(17)
O3	8*d*	0.1309(5)	0.0902(13)	0.3261(6)	1.23(17)
O4	8*d*	0.2102(5)	0.2081(13)	0.1713(6)	0.78(14)
O5	8*d*	0.3848(5)	0.2672(14)	0.2078(6)	1.24(16)
O6	8*d*	0.4685(5)	0.1374(13)	0.3626(6)	1.12(16)
O7	8*d*	0.3234(4)	0.0424(12)	0.0623(6)	0.91(16)
O8	8*d*	0.2936(5)	0.0036(13)	0.3064(7)	1.48(16)
O9	8*d*	0.0791(4)	0.3968(14)	0.2119(6)	0.74(13)

Note. Space group *Pbcn* (No.60), orthorhombic; cell parameters: $a = 18.7599(10)$ Å, $b = 7.0638(4)$ Å, $c = 14.9548(7)$ Å; $R_B = 4.26\%$, $R_p = 3.30\%$ for neutrons; $R_B = 4.28\%$, $R_p = 4.91\%$ for X rays.

TABLE 4
U–O Distances and Their Bond Valences in the Various Uranium Environments for the Cesium Uranates

	Bond	Length (Å)	Valence *s*
		Cs_2UO_4	
2×	U–O2	1.914(2)	1.509
4×	U–O1	2.196(1)	0.724
			5.914
		$Cs_4U_5O_{17}$	
2×	U1–O6	1.784(9)	1.913
2×	U1–O9	2.297(8)	0.541
	U1–O1	2.340(15)	0.477
2×	U1–O5	2.446(9)	0.354
			6.093
	U2–O3	1.847(10)	1.721
	U2–O2	1.866(10)	1.658
	U2–O1	2.206(6)	0.704
	U2–O5	2.214(8)	0.690
	U2–O4	2.260(10)	0.603
	U2–O9	2.295(8)	0.549
			5.925
	U3–O8	1.825(11)	1.787
	U3–O7	1.852(9)	1.702
	U3–O5	2.196(9)	0.722
	U3–O9	2.270(8)	0.584
	U3–O4	2.307(8)	0.529
	U3–O4	2.310(9)	0.523
			5.847
		$Cs_2U_2O_7$	
	U–O1	1.807(6)	1.844
	U–O2	1.835(5)	1.755
	U–O4	2.158(7)	0.807
2×	U–O3	2.245(2)	0.629
	U–O3	2.345(5)	0.473
			6.137
		$Cs_2U_4O_{12}$	
6×	U1–O5	2.134(18)	0.907
			5.442
	U2–O1	1.923(20)	1.481
	U2–O3	2.031(23)	1.152
	U2–O6	2.062(19)	1.061
	U2–O5	2.066(18)	1.049
	U2–O3	2.233(22)	0.651
	U2–O4	2.261(20)	0.601
			5.995
2×	U3–O8	1.952(21)	1.391
2×	U3–O7	2.169(16)	0.782
2×	U3–O6	2.204(19)	0.708
			5.762
	U4–O2	1.958(16)	1.425
	U4–O4	1.973(17)	1.379
	U4–O7	2.273(17)	0.610
	U4–O7	2.354(19)	0.484
	U4–O1	2.383(22)	0.445
	U4–O2	2.429(19)	0.391
	U4–O8	2.454(17)	0.364
			5.098

TABLE 5
XPS Data Obtained on Cs_2UO_4

U4$f_{7/2}$ (eV)	380.7
U4$f_{5/2}$ (eV)	391.6
FWHM (eV)	2.3
Satellite separation (eV)	10.0
Satellite FWHM (eV)	3.0
O1*s* (eV)	530.8
FWHM (eV)	3.1
Cs3*d* (eV)	724.3
FWHM (eV)	2.1

Note. This data is to be compared to the XPS data obtained on the other monovalent uranates (found in (1) and Fig. 3). The large width and high BE of the O1*s* peak are a consequence of hydratation of the sample as seen by the development of an important OH-contribution to the O1*s* peak.

longer axial and shorter equatorial bonds. Although the uranyl structure is common in many uranium compounds, some show symmetrical uranium environments, which are described as 'uranate' structures. For these, equal or nearly equal lengths are found for all U–O bonds. Local environments comparable to the "uranate" and "uranyl" groups are found in most actinide ternary oxides and we can therefore speak of "actinyl" and "actinate" or "-yl" and "-ate" structures in short.

The U^{VI} monovalent nature of these compounds is confirmed by the BVS calculations as displayed in Table 4. For all uranium atoms, a BVS close to 6 is found. This result ensures the accuracy of the atomic positions determined, as the BVS is very sensitive to variations in the U–O distances.

The crystallographic structures of the monovalent cesium uranates are related to each other. Concerning the heavy atoms, all structures form layers of cesium and UO_n ($n = 6$ or 7) polyhedra. For $Cs_2U_2O_7$, this layered structure is observed in Fig. 5b. When more cesium is introduced, the cesium layers become double for Cs_2UO_4 (Fig. 5a), while an undulated layer is produced when the Cs/U ratio is lower in $Cs_4U_5O_{17}$ (Fig. 5c).

Figure 1 shows the XANES spectra for all samples and some reference compounds. Due to the difficulty in obtaining a pure, stable UO_2^+ reference sample, we used the data obtained for the isostructural moiety, NpO_2^+ (16). Since the U and Np L_{III}-edge data were calibrated against their respective Ac(IV)O_2 powder XANES spectra (nearly identical), the data in Fig. 1 allows for direct comparison between the U and Np spectra, because it is displayed on a relative energy scale. Also listed in Fig. 1 is the calculated formal valence and structural moiety ("-yl" for uranyl, "-ate" for uranate) for each sample. Both properties are known to have their influence on the XANES structure, although their contributions are hard to decouple (17).

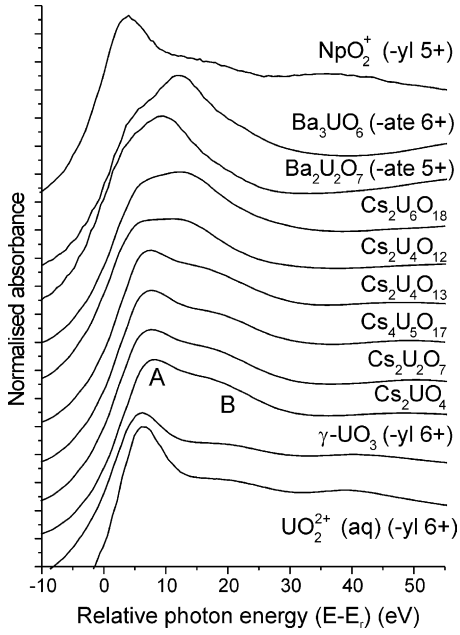

FIG. 1. XANES spectra for the different cesium uranates. The difference between the monovalent and multivalent uranates is immediately obvious. For comparison, the spectra of $Cs_2U_4O_{13}$ and $Cs_2U_6O_{18}$ are also included. As reference spectra, we have included Ba_3UO_6 (U^{6+} "uranate"), $Ba_2U_2O_7$ (U^{5+} 'uranate'), UO_2^{2+} and γ-UO_3 (U^{6+} 'uranyl') and the 5+ neptunyl (NpO_2^+) spectrum. The neptunyl spectrum was used because no free 'uranyl' UO_2^+ spectra are available. Because all spectra are displayed relative to their absorption edge energy ($E_r = 17,166$ eV for UL_{III}), a comparison between the NpO_2^+ spectrum and the uranium XANES is possible.

The four reference compounds NpO_2^+, UO_2^{2+}, $Ba_2U_2O_7$ and Ba_3UO_6 provide a nice comprehensive representation of the actinyl +5, +6 and uranate +5, +6 moieties, respectively. The L_{III} absorption edge of the actinides arises from the formally allowed $2p_{3/2} \rightarrow 6d$ electronic transition. The actinyl spectra are dominated by a sharp white line (A) followed by a shoulder (B, MS resonance) on the high-energy side. On the other hand, the XANES spectra for the uranate species ($Ba_2U_2O_7$ and Ba_3UO_6) display almost a reverse pattern to that observed in the actinyl compounds. That is, an intense white line with a shoulder on the low-energy side is observed. Upon initial inspection, the XANES data indicate that the formally (+6) cesium uranates most closely resemble the uranyl UO_2^{2+}(aq) sample, although the white line features are shifted and less pronounced.

The EXAFS spectra of all monovalent cesium uranates look similar, which agrees with the observation that the average crystallographic environments of all uranium atoms in these compounds are very much alike. The EXAFS data were modeled using the simplified EXAFS equation (11). This equation requires parameters concerning the mean U–O distances. The experimental data could be accurately modeled using three oxygen "shells". For Cs_2UO_4, values of 1.83, 2.19 and 2.34 Å are derived, while for $Cs_2U_2O_7$, the distances used were 1.84, 2.20 and 2.36 Å. For $Cs_4U_5O_{17}$, the values were 1.83, 2.18 and 2.31 Å. We can compare these values to the bond lengths d extracted from the crystal structures. This is done in Fig. 2, where the crosses denote the U–O distances as derived from the crystal structure (Table 4) and the lines indicate the values adopted to model the EXAFS data. The agreement is fair for $Cs_4U_5O_{17}$ and $Cs_2U_2O_7$, but less good for Cs_2UO_4. In general, a repartition of the distances in two groups, the second one being modeled with two separate U–O lengths, is an acceptable representation for these uranates and supports the coherence of the data. For Cs_2UO_4, values of 1.83 Å, 2.19 Å and 2.34 Å for the three U–O shell sizes are derived, while for $Cs_2U_2O_7$, the distances used were 1.84, 2.20 and 2.36 Å. For $Cs_4U_5O_{17}$, the values were 1.83, 2.18 and 2.31 Å. If we divide the bond lengths d extracted from the crystal structure into three groups: $d < 2.0$, $2.0\,\text{Å} < d < 2.25\,\text{Å}$ and $d > 2.25$ Å and take the mean bond length for each group, the values obtained are 1.82, 2.22 and 2.35 Å for $Cs_2U_2O_7$, in close agreement with the values used in the EXAFS model for this compound. For $Cs_4U_5O_{17}$, the mean distances for each group are 1.83, 2.21 and 2.33 Å, again close to the parameter values used to model the EXAFS spectrum. The mean values for each group are indicated in Fig. 2 as black rectangles. The repartition of the bond lengths in three groups is based on the fact that the first group contains the axial oxygen atoms, while the other two contain the equatorial oxygens. For Cs_2UO_4, the first-shell distance of 1.83 Å is in less good

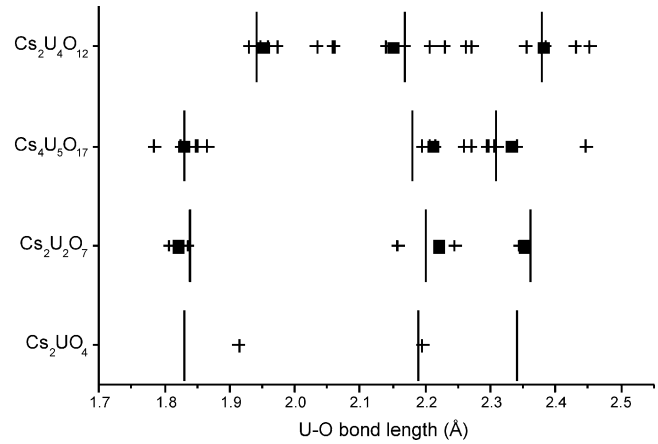

FIG. 2. Comparison between the U–O distances derived from the structure refinements and the EXAFS modeling parameters. The crystallographic U–O distances are indicated as crosses in the graph. The distances d can be divided in three groups ($d < 2.0$, $2.0\,\text{Å} < d < 2.25\,\text{Å}$ and $d > 2.25$ Å) and the mean distances for each group is shown as a black square. A good agreement of these means with the EXAFS modeling parameters (indicated as vertical lines) is obtained for $Cs_2U_2O_7$, $Cs_4U_5O_{17}$ and $Cs_2U_4O_{12}$. For Cs_2UO_4, the agreement is less good.

agreement with the axial U–O distance of 1.916 Å, which may be due to the much more symmetrical uranium environments in this compound and the absence of an actual "third shell". However, modeling the EXAFS data of this compound with only two shells brings the axial U–O distances from EXAFS and crystal structure in closer agreement, but does not produce satisfying results for the equatorial distances. It should be made clear that EXAFS perceives a structure from the perspective of a central atom absorber, with the photoelectron scattering off the nearest neighbors, which is different from diffraction. As a result, the techniques will be sensitive to slightly different structural effects. It is also possible that some hydrolysis of the sample had occurred during transport, which could explain the anomaly.

As discussed in (1), the XPS spectra of all monovalent uranates show a typical U^{VI} signature: U4$f_{7/2}$ peaks at 380.7–381.3 eV (<2 eV FWHM) with satellites at distances of 4 and 10 eV to the main peak. The spectral data obtained on Cs_2UO_4 (see Table 5) follow all the trends established in (1). Their U4*f* peaks have a somewhat larger width (2.3 eV compared to 1.9 eV), which is probably due to some hydratation of this compound. This is reflected in the O1*s* peak position and width. The OH-related high binding energy shoulder of this peak has developed markedly and causes the peak position to be higher than found for the other uranates, in conjunction with a much larger FWHM (3.1 eV instead of 2.2 eV). The results on this compound follow the trend for the U4*f* BE to increase with smaller Cs/U ratio, as shown in Fig. 3. A similar evolution was also observed by the authors for other alkali metals (Na, K and Rb) as seen in Fig. 3. This small shift of the U4*f* BE cannot be directly related to the crystal structure variations.

Comparing the obtained data to previous XPS measurements on Cs_2UO_4, we see that our binding energy values are somewhat lower than those found in (18), taking into account the different values for the C1*s* position adopted (284.8 eV in (18) and 285.0 eV here). In view of the established trend of the U4*f* position with Cs/U ratio, our values are in better agreement.

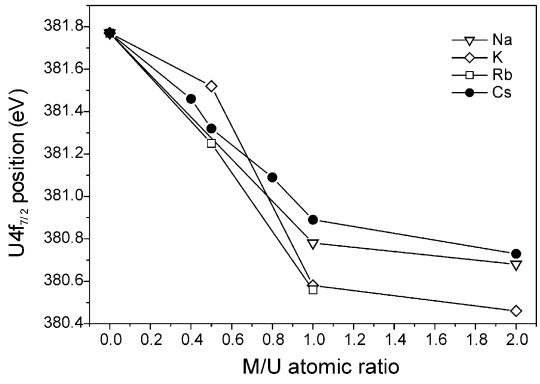

FIG. 3. U4$f_{7/2}$ binding energy in function of the M/U ratio (M = Na, K, Rb, Cs) in the cesium uranates (1) and other alkali metal uranates. All values have been calibrated against the 285.0 eV position for the C1*s* peak from adventitious carbon. The value at M/U = 0 is the U4*f* BE of UO_3, which is also a uranyl compound.

3.2. *Mixed Valence Compound: $Cs_2U_4O_{12}$*

The multivalent $Cs_2U_4O_{12}$ has four crystallographically different uranium positions, as seen in Table 6. The U1 site has a completely symmetrical ('uranate'-type) environment of six O atoms and a multiplicity of 3. The U2 and U4 sites both have multiplicities of 18. The U4 has a seven-fold co-ordination, while the U2 has a six-fold. For the U3 a co-ordination 6 is observed with a multiplicity of 9. From the electrostatic valences (see Table 4), it can be deduced that the U1 and U4 sites contain U^{5+} ions, while the others are U^{6+}. This arrangement does not produce a completely ordered structure, as will be discussed later.

The bond lengths in this compound show much more symmetrical uranium environments than in the monovalent uranates, with longer "axial bonds" that are only slightly shorter than the equatorial ones (see Table 4), except for the seven-coordinated U4. Due to its higher co-ordination, there is a larger difference between the axial and equatorial bond lengths, similar as found for U1 in $Cs_4U_5O_{17}$. Such more symmetrical environments can also be observed for $Cs_2U_6O_{18}$, also a mixed valence compound. The refinement results did not provide entirely satisfying results for this compound, however, and it was therefore not included in this study.

TABLE 6
Final Refined Lattice Parameters, Fractional Coordinates, and Isotropic Temperature Factors B_{iso} of $Cs_2U_4O_{12}$

Atom	Site	x/a	y/a	z/c	B_{iso}(Å^2)
Cs1	18*f*	0.1615(5)	0.3371(6)	0.2124(3)	2.73(11)
Cs2	6*c*	0	0	0.1463(5)	0.80(19)
U1	3*b*	0	0	$\frac{1}{2}$	0.46(15)
U2	18*f*	0.2358(2)	0.4936(3)	0.0019(2)	0.18(5)
U3	9*d*	$\frac{1}{2}$	0	$\frac{1}{2}$	0.30(7)
U4	18*f*	0.2252(2)	0.2389(2)	−0.0131(1)	0.34(5)
O1	18*f*	0.0964(12)	0.4015(12)	0.0214(7)	0.67(27)
O2	18*f*	0.0772(12)	0.1882(11)	0.0583(8)	1.02(27)
O3	18*f*	0.9187(14)	0.8677(15)	0.6836(9)	1.43(32)
O4	18*f*	0.8987(13)	0.2696(12)	0.9703(9)	1.00(30)
O5	18*f*	0.7447(14)	0.4670(13)	0.8943(9)	1.18(28)
O6	18*f*	0.7872(12)	0.5306(14)	0.1034(9)	1.29(29)
O7	18*f*	0.5701(11)	0.0857(11)	0.4065(8)	0.84(29)
O8	18*f*	0.2763(12)	0.3208(13)	0.8727(9)	1.20(30)

Note. Space group $R\bar{3}$ (No.148), trigonal (hexagonal axes); cell parameters: $a = 15.4207(6)$ Å, $c = 19.1762(11)$ Å; $R_B = 5.32\%$, $R_p = 4.27\%$ for neutrons; $R_B = 4.40\%$, $R_p = 5.68\%$ for X-rays.

The spectra for the mixed valence compounds, $Cs_2U_4O_{12}$ and $Cs_2U_6O_{18}$, contain two XANES peaks which appear to be intermediate in form to similar features noted in the pure -yl and -ate spectra. Based on the apparent shift in intensity and position of the two prominent XANES features (A and B in Fig. 1) between the pure -yl and -ate spectra, and the knowledge of structural heterogeneity in the Cs uranates (i.e., a mixture of -yl and -ate sites), we developed a phenomenological curve fitting procedure to quantify the relative contributions of each oxidation state (5/6) and structural moiety (-yl/-ate) in the mixed valence $Cs_2U_4O_{12}$.

First, the spectra for NpO_2^+(aq), UO_2^{2+}(aq), $Ba_2U_2O_7$ and Ba_3UO_6 were deconvolved and fit using a combination of two Voigt functions (corresponding to the white line + weaker shoulder) plus an arctangent function to simulate the absorption edge jump. This was done in order to quantify the spectral features A and B (intensities, positions, and widths) for these end point spectra.

Next an assumption was made that hypothetical XANES spectra for pure U^V or U^{VI} compounds containing a mixture of -ate or -yl sites present could be constructed by taking a weighted average of the parameters (intensities, positions, and widths) obtained for features A and B in the pure end point spectra. In other words, these spectral features are in fact highly dependent on local structure. This is a plausible approach because numerous XANES features have previously been shown to originate from scattering resonances that correspond to specific local structures (19). Furthermore, the positions and intensities of these resonances can be correlated directly to changes in the local bond lengths. In the present work, we are attempting to test the validity of such relationships at a purely phenomenological level.

Thus in order to create several theoretical reference spectra lying in the continuum between -ate and -yl structures for each oxidation state, combination spectra were reproduced where the amplitudes, positions, and widths of features A and B from the pure uranyl and uranate models were combined using designated -yl and -ate weightings of 25%, 50%, and 75% (respectively).

The mixed valence spectra were then fit using binary combinations of the following +5 and +6 components: (100% -yl), (25% -ate/75% -yl), (50% -ate/50% -yl), (75% -ate/25% -yl) and (100% -ate). The best fit results of this procedure are shown in Fig. 4 for $Cs_2U_4O_{12}$. The best fit is obtained using a linear combination of a 100% -yl (+5) component for the U^V oxidation state and the mixed 75% -ate/25% -yl component for the U^{VI} oxidation state. Using these components, we find a +6/+5 ratio of 60%/40% in the $Cs_2U_4O_{12}$ sample (and 81%/19% in the $Cs_2U_6O_{18}$) sample, in reasonable agreement with the formal valences of +5.5 (and +5.67).

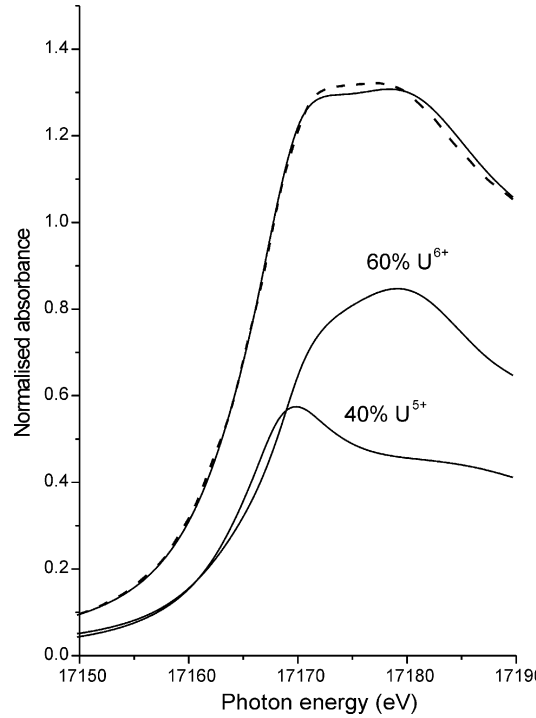

FIG. 4. Deconvolution of the $Cs_2U_4O_{12}$ XANES spectrum with two components derived from the reference data. The U^{6+} peak is built from 75% uranate environment (from the Ba_3UO_6 spectrum) and 25% uranyl environment (from the γ-UO_3 spectrum). The U^{5+} spectrum is taken from the uranyl spectrum of the "free $(U^V)O_2^+$" ion, which is in fact a shifted neptunyl spectrum, since no free uranyl 5+ spectrum is available. The dotted line shows the experimental data.

For the EXAFS data modelling, again a set of three oxygen shells were introduced at distances of 1.94, 2.17 and 2.38 Å. The comparison with the U–O bond lengths from the refinement is again displayed in Fig. 2. It can be seen that the agreement is good for this compound. EXAFS shows the mean of all uranium environments, which requires that the modelization parameters represent many individual distances at the same time. The U–O bond lengths can again be divided into three groups as was done for the monovalent uranates and mean bond lengths for each group of 1.95, 2.15 and 2.38 Å are calculated.

From XPS, deconvolution of the U4*f* photoelectron peak has lead to the conclusion that U^V and U^{VI} are the uranium valence states in $Cs_2U_4O_{12}$ (1). On the basis of the peak areas, it was deduced that uranium assumes 48% U^V and 52% U^{VI} character.

4. DISCUSSION

It is important to notice the coherence between the information extracted from each measurement technique. The combined interpretation of this wealth of data leads to a better understanding of the local uranium environment.

4.1. Monovalent Cesium Uranates

The presence of alternating layers of uranium (UO_6 or UO_7 polyhedrals) and cesium atoms in the crystal structures (see Fig. 5) is the cause for the longer axial bonds found in the cesium uranates compared to e.g., UO_3. The cesium atoms are bound to the axial oxygen ligands and their attraction on these oxygen atoms causes the distance to the uranium atom to increase. For Cs_2UO_4, the double cesium layers in-between two uranium layers cause even larger axial bond lengths. On the other hand, this is compensated by a decrease in the equatorial oxygen–uranium distances or an increase in the uranium coordination from 6 to 7. This results in total electrostatic valences that remain close to 6, as would be expected (see Table 4).

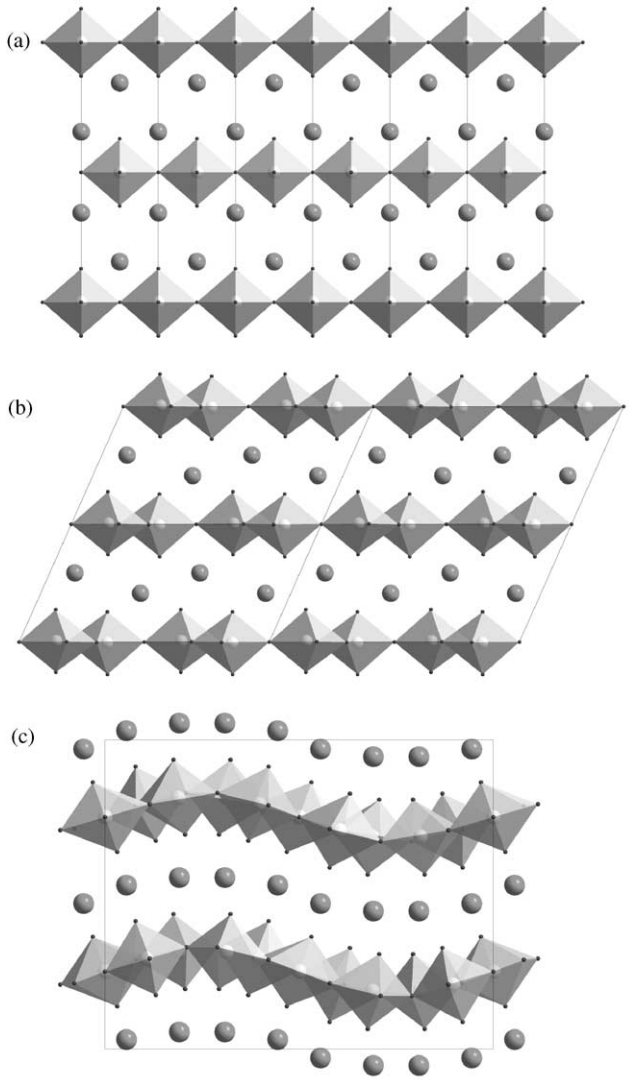

FIG. 5. Views of the crystal structures of (a) Cs_2UO_4 in the $\langle 100 \rangle$-direction, (b) $Cs_2U_2O_7$ in the $\langle 010 \rangle$-direction and (c) $Cs_4U_5O_{17}$ in the $\langle 010 \rangle$-direction. Inside the polyhedra, having oxygen atoms at their corners, are the uranium atoms. The isolated atoms in between the layers of polyhedra are the cesium atoms. The evolution of the layered crystal structure with the cesium content of the uranates is clearly observable.

This agreement between the bond valence sums as determined in the formalism of Zachariasen and the actual valences present, is very encouraging. The general formula postulated by Brown *et al.* (5) does not give satisfying results because the contribution of the axial U–O bonds is systematically overestimated. The reason for this lies in the use of a constant value for b where Zachariasen allows the value to vary for the very short axial U–O distances. These bond lengths are very short indeed, compared to the other ligands. This is difficult to understand in view of the large spatial extent of the U6*p* orbitals, which should produce an important electrostatic repulsion at short U–O distances. The explanation is given by relativistic molecular orbital calculations, revealing the important attractive interaction between the U5*f* orbital and the O2*p*, while the U6*p* orbital, in spite of its large overlap with the O2*p*, has a smaller effect (20, 21). This peculiar behavior of the U–O bonding is the most probable reason why the general formula of Brown *et al.* is less applicable for the short axial U–O distances in uranyl-type environments. This is illustrated by the fact that the application of the Brown parameters to assess the valence of U in γ-UO_3 yields values of 6.42 and 6.16 for the two U positions; while the Zachariasen parameters give 5.90 and 6.01.

The U valence in the monovalent uranates is confirmed by XPS, for which only well-defined U^{VI} U4*f* positions are found. Their BEs are lower than found for γ-UO_3 (1). This lower BE compared to UO_3, is explained by the longer axial bonds in the uranyl environments found in the uranates compared to UO_3. Although the total electrostatic valence of the uranium atoms is the same in all these compounds (all U^{6+}), the axial bond lengths have a more important influence on the BE than the equatorial oxygens. This is mainly because the axial U–O bonds have a large degree of covalence in which the 5*f* electrons invested in the bond by the central uranium atom, to a large degree (40%), retain their 5*f* character (21, 22). In a purely ionic picture, these electrons would have become of O2*p* signature. As the axial U–O bond lengths decrease, charge is transferred away from the uranium atom as well as from the axial oxygen atoms. As a consequence, the highest uranium BEs are associated with the smallest axial U–O distances (8). In (1), it is also mentioned that the splitting of the U6$p_{3/2}$ line could not be accurately observed due to the interference with the O2*p* level. Thanks to the presently available crystal structures, it can now be assumed that this splitting will be very limited, since the crystal field responsible for this splitting will be very limited because of the long axial U–O distances (9).

4.2. Mixed Valence Uranate

For the multivalent compound, discussion of the results is somewhat more tedious. The crystal structure and BVS calculations lead to the conclusion that two U sites contain U^{5+} (U1 and U4) and two contain U^{6+} (U2 and U3). Taking into account the multiplicities, this gives a U^{5+}–U^{6+} ratio of 44%/56%, in agreement with the XPS results on this ratio (48%/52%) and the deconvolution of the XANES signal (40%/60%). However, the assignment of these single valences to unique crystal sites leads to problems in the charge balance. With multiplicities of 3 and 18 for the U^{5+} sites and 9 and 18 for the U^{6+} sites, a total positive charge of 291 units is present in the crystal if the cesium ions are assigned a +1 charge. However, only 288 negative charge units are brought in by the 144 oxygen atoms in the unit lattice. A disordering of charges on some sites is probable. The simplest distribution in good agreement with the calculated bond valences corresponds to an ordered distribution of U^{5+} on the U1 and U4 sites, of U^{6+} on the U2 site and to an average distribution of one U^{5+} and two U^{6+} on the U3 site (4). A similar reasoning was put forward to account for the intermediate valence of Mo in $La_7Mo_7O_{30}$ (23). It is remarkable that the assumption of U^{4+} being present on the U1 site, brings the charges in balance, but this is in contradiction with all other data. Nor in XPS, nor in XANES, any indication was found for presence of U^{IV} and the local U1 environment leads to a BVS of 5.334.

The symmetric (''uranate'') environment of the U1 site cannot be regarded as an indication for it having a valence of +4, since ''uranate'' environments have also been observed for U^{5+} ($Ba_2U_2O_7$) and U^{6+} (Ba_3UO_6). Even in the case of $Cs_2U_4O_{12}$, the other uranium environments cannot be regarded as typical of uranyl. The axial bond lengths for the U2 and U3 sites are hardly distinguishable from the equatorial distances. This is also the reason why the XANES data had to be fitted with a 75% ''uranate'' peak for the U^{VI} component. For the U^{V} component, a ''uranyl'' peak could be used, because this component is dominated by the contribution from the U4 site (multiplicity of 18 compared to 3 for U1), where the higher coordination produces larger differences between the equatorial and axial bond lengths. The longer axial U–O distances are confirmed by the modeling parameters for the EXAFS data. A possible explanation for these longer axial U–O bond lengths could lie in its crystal structure. While the monovalent uranates show layered structures, in which asymmetrical environments are easily formed, the multivalent $Cs_2U_4O_{12}$ does not contain separated UO_n and Cs layers, but rather forms a complex three-dimensional network-type structure (4).

It is conceivable that the symmetries of the uranium sites have their influence on the bonding and hence on the valence. From Molecular Orbital (MO) calculations, it is known that the secondary ligands have an influence on the participation of the 5*f* electrons in the axial U–O bonds (24) and on the electrical field gradient at the U position (21). The large distances between the U atom and its equatorial oxygens prevent strong covalent bonding interaction with these equatorial ligands. In fact, their influence can be modeled by a simple electrostatic field. This crystal field determines to some extent the 5*f* and 6*d* character of the UO_2^{2+} bonding or, in other words, the covalence of the axial U–O bonds. Because the BVS interpretation in function of integer valences is based on the assumption of ionic bonding, the symmetry of the equatorial oxygens will play its role, although it remains unclear what exactly that role is. Further studies of the local uranium moieties in -yl and -ate configurations with associated MO or cluster calculations is required.

Difficulties with assigning valences in uranates and other uranium compounds have been reported before in mixed valence uranium compounds. A good example is MUO_3, with M = Na, K, Rb. Formally, these structures have only one valence, namely U^{V}. Their crystal structures are based on a perovskite structure with only one crystallographic position for U (for KUO_3 (25), $NaUO_3$ (26, 27), $RbUO_3$ (28)). As far as these two observations are concerned, there is no objection against classifying the MUO_3 as monovalent compounds. However, the XPS spectra of these uranates clearly show doublet structures for the U4*f* peaks, indicating a mixed valence (for $NaUO_3$ (29) and similar results were observed by the authors on KUO_3 and $RbUO_3$). The observed discrepancy bears much resemblance to the situation encountered for $BaBiO_3$. Formally, Bi has a valence of +4, but it was shown on various occasions that a disproportionation in Bi^{3+} and Bi^{5+} occurs, also on the basis of neutron diffraction data refinement (30,31) and bond length–bond valence considerations (32), XPS data (33) and EXAFS measurements (34).

The assignment of valences in U_3O_8 is also a long-lasting point of discussion. The crystal structure found for α-U_3O_8 (35) does not show any important differences in uranium environment for the two U sites. They can be assigned valences of 5.33 by BVS calculation. In XPS, the compound is identified as a multivalent compound with U^{IV} and U^{VI} valences (29). It is unclear if the mixed valence character of this oxide as seen with XPS is a consequence of final-state effects or is rather due to actual mixed or intermediate valence on the crystallographic level or the electronic level.

5. CONCLUSION

The local uranium environment was studied in four cesium uranates: Cs_2UO_4, $Cs_2U_2O_7$, $Cs_4U_5O_{17}$ and $Cs_2U_4O_{12}$. It was shown that, from their crystal structure

as determined by Rietveld refinement of the neutron and X-ray diffractograms, an assessment can be made of the uranium valences present through Bond Valence Sum (BVS) calculations. For these BVS determinations, the formalism of Zachariasen has to be applied, because the short axial U–O distances in the 'uranyl'-type uranium environments are systematically overestimated when the parameters of Brown *et al*. and Brese *et al*. are used.

It was demonstrated that the monovalent cesium uranates all have uranyl-type uranium environments, both from the crystal structure determinations and the XANES data. The interatomic distances as determined from the refinements, are shown to be in agreement with the EXAFS data modeling. From these distances, BVS calculations all lead to uranium valences close to 6, which is in agreement with the XPS results. For these, narrow U4f peaks at the U^{VI} position were found for all monovalent cesium uranates.

For $Cs_2U_4O_{12}$, which is a multivalent cesium uranate, the valence determination from the crystal structure yields valences of $+5$ and $+6$, in agreement with the deconvolution results of the XPS and XANES spectra. However, the assignment of these valences demands for some degree of disorder on some or all of the uranium sites in the lattice, in order to balance the charges. We propose an ordered distribution of U^{5+} on the U1 and U4 sites, of U^{6+} on the U2 site and an average distribution of one U^{5+} and two U^{6+} on the U3 site. In $Cs_2U_4O_{12}$, the uranium environments are much more symmetric than in the monovalent uranates, which is confirmed by the interpretation of the XANES and EXAFS results.

It can be concluded that multivalent cesium uranates specifically and uranates that contain other valences than just U^{VI} in general, show a rather peculiar valence behavior. It is probable that the 5*f* and 6*p* electrons in uranium and their interaction with the O2*p* level are the cause for this. In order to understand the behavior of these electrons, the local uranium environment is of primordial importance.

ACKNOWLEDGMENTS

The authors thank Dr. E. Suard at the Institut Laue-Langevin in Grenoble for her help with the neutron diffraction experiments and Prof. Dr. H. Terryn and Ing. O. Steenhaut from the University of Brussels for the use of their XPS equipment. The authors are gratefully acknowledging the permission of Dr. L.R. Morss (Argonne National Laboratory) to use his barium uranate samples. Furthermore, the authors acknowledge the work of E. Sylwester in the XAS data-analysis.

REFERENCES

1. S. Van Den Berghe, J. P. Laval, B. Gaudreau, H. Terryn, and M. Verwerft, *J. Nucl. Mater*. **277,** 28 (2000).
2. A. B. Van Egmond, Investigations on cesium uranates and related compounds, Technical Report RCN-246, RCN, Petten, 1976.
3. F. C. Mijlhoff, D. J. W Ijdo, and E. H. P. Cordfunke, *J. Solid State Chem*. **102,** 299 (1993).
4. S. Van Den Berghe, J.-P. Laval, M. Verwerft, B. Gaudreau, and E. Suard, *Sol. State Sciences*, to be submitted.
5. I. D. Brown and D. Altermatt, *Acta Crystallogr. B* **41,** 244 (1985).
6. W. H. Zachariasen, *J. Less-Comm. Metals* **62,** 1 (1978).
7. B. W. Veal, D. J. Lam, W. T. Carnall, and H. R. Hoekstra, *Phys. Rev. B* **12,** 5651 (1975).
8. B. W. Veal and D. J. Lam, *Photoemission spectra*, "Gmelin Handbook of Inorganic Chemistry" Vol. Suppl. A5, Chap. 4, pp. 176–210, Springer-Verlag, Berlin, 1982.
9. G. C. Allen, A. J. Griffiths, and B. J. Lee, *Transition Metal Chem*. **3,** 229 (1978).
10. J. Rodriguez-Carjaval, "Fullprof," 2000, multipattern version.
11. R. Prins and D. E. Koningsberger, "X-Ray Absorption: Principles, Applications, Techniques for EX-AFS, SEXAFS and XANES," Wiley-Interscience, New York, 1988.
12. J. M. de Leon, J. J. Rehr, S. Zabinsky, and R. C. Albers, *Phys. Rev. B* **44,** 4146 (1991).
13. B. Ravel, "ATOMS, a Program to Generate Atom Lists for XAFS Analysis from Crystallographic Data," University of Washington, Seattle, WA, 1996.
14. N. E. Brese and M. O'Keeffe, *Acta Crystallogr. B* **47,** 192 (1991).
15. E. M. Van Wezenbeek, "Relativistic Effects in Atoms and in Uranium Compounds," Ph.D. thesis, Vrije Universiteit, Amsterdam, 1992.
16. P. G. Allen, J. J. Bucher, D. K. Shuh, N. M. Edelstein, and T. Reich, *Inorg. Chem*. **36,** 4676 (1997).
17. C. Den Auwer, E. Simoni, S. D. Conradson, J. Mustre de Leon, P. Moisy, and A. Béres, *C.R. Acad. Sci. Paris* Sér. **IIc,** 327 (2000).
18. A. H. Al Rayyes and C. Ronneau, *Radiochim. Acta* **54,** 189 (1991).
19. P. G. Allen, D. K. Shuh, J. J. Bucher, N. M. Edelstein, C. E.-A. Palmer, L. N. Marquez, E. A. Hudson, R. J. Silva, and S. N. Nguyen, *Radiochim. Acta* **75,** 47 (1997).
20. L. E. Cox, *J. Electron Spectr. Rel. Phenon*. **26,** 167 (1982).
21. W. A. de Jong, L. Visscher, and W. C. Nieuwpoort, *J. Mol. Struct. (Theochem)* **458,** 41 (1999).
22. E. M. Van Wezenbeek, E. J. Baerends, and J. G. Snijders, *Theor. Chim. Acta* **81,** 139 (1991).
23. F. Goutenoire, R. Retoux, E. Suard, and P. Lacorre, *J. Solid State Chem*. **142,** 228 (1999).
24. P. F. Walch and D. E. Ellis, *J. Chem. Phys*. **65,** 2387 (1976).
25. P. G. Dickens and A. V. Powell, *J. Mater. Chem*. **1,** 137 (1991).
26. S. F. Bartram and R. E. Fryxell, *J. Inorg. Nucl. Chem*. **32,** 3701 (1970).
27. A. M. Chippindale, P. G. Dickens, and W. T. A. Harrison, *J. Solid State Chem*. **78,** 256 (1989).
28. W. Ruedorff, S. Kemmler, and H. Leutner, *Angew. Chem*. **74,** 429 (1962).
29. G. C. Allen, J. A. Crofts, M. T. Curtis, and P. M. Tucker, *J. Chem. Soc. Dalton Trans*. **1974,** 1296 (1974).
30. D. E. Cox and A. W. Sleight, *Solid State Commun*. **19,** 969 (1976).
31. C. Chaillout, J. P. Remeika, A. Santoro, and M. Marezio, *Solid State Commun*. **56,** 829 (1985).
32. N. K. McGuire and M. O'Keeffe, *Solid State Commun*. **52,** 433 (1984).
33. G. K. Wertheim, J. P. Remeika, and D. N. E. Buchanan, *Phys. Rev. B* **26,** 2120 (1982).
34. A. Balzarotti, A. P. Menushenkov, N. Motta, and J. Purans, *Solid State Commun*. **49,** 887 (1984).
35. B. O. Loopstra, *J. Inorg. Nucl. Chem*. **39,** 75 (1977).